

Concrete at early ages analysis

Theory and application

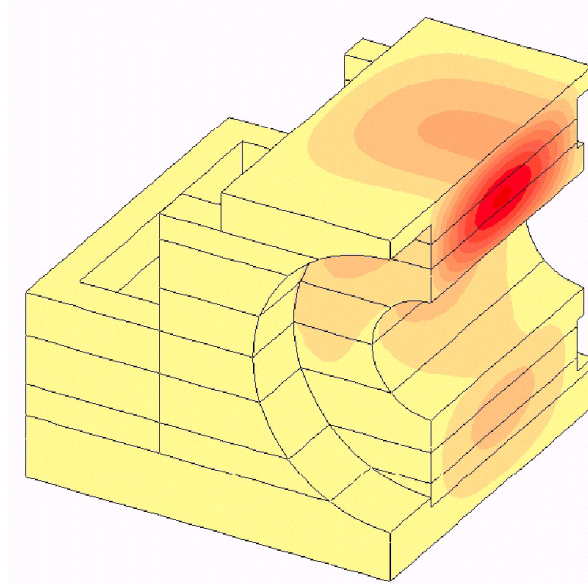


figure 1: Model for the extension of the Monaco's dike (itech expertise with courtesy of BEC-DRAGADOS-FCC)

Table of content

1.	BENEFIT OF MODELLING EARLY AGE CONCRETE	3
2.	MODULE TEXO	3
2.1.	<i>Theoretical and experimental aspects</i>	3
2.2.	<i>The "QAB" calorimetric test</i>	4
2.3.	<i>Boundary conditions</i>	5
3.	MODULE MEXO	6
3.1.	<i>Theoretical and experimental aspects</i>	6
3.2.	<i>Concrete hardening</i>	7
3.3.	<i>Coefficient of dilatation/chemical shrinkage</i>	8
4.	RESULT OF A "QAB" CALORIMETRIC TEST	9
5.	TEXO-MEXO IN EXAMPLE: CONCRETING STAGES AND THERMAL TREATMENT	11
5.1.	<i>Introduction</i>	11
5.2.	<i>Some results of the TEXO analysis</i>	13
5.3.	<i>Some results of the MEXO analysis</i>	16
6.	BIBLIOGRAPHICAL RÉFÉRENCES	18

1. BENEFIT OF MODELLING EARLY AGE CONCRETE

The hydration reaction of the cement is highly exothermic. The concrete hardens by exposure to rising temperature, which may reach as high as 50°C within solid structures. Cement hydration represents a thermo-activated reaction, which signifies that the speed of this chemical reaction increases with temperature.

Moreover, concrete is an aging material, i.e. its mechanical properties (modulus of elasticity, strength) evolve as a function of the level of progress in the cement hydration reaction. The consumption of water during the hydration reaction leads to chemical shrinkage coupled with capillary shrinkage. When prevented, these various shrinkages, along with the temperature gradients, induce stresses of such intensity that they may wind up exceeding the tensile stress of the material undergoing maturation and hence lead to cracking. This cracking, in turn, affects the durability of concrete structures.

The TEXO and MEXO modules have been developed to enable modeling these phenomena. TEXO serves to compute both the temperature and degree of hydration fields, used to express the material's state of hardening. These results are then inputted into the MEXO module in order to determine the displacement and stress fields, in the aim of predicting the risk of cracking at early age.

2. MODULE TEXO

2.1. Theoretical and experimental aspects

The TEXO module is primarily a computation module intended for the simultaneous resolution of the heat equation:

$$C \frac{dT}{dt} = -\text{div}q + I \frac{dx}{dt} \quad (1)$$

with: $q = -K \times \text{grad}T$

and the macroscopic kinetic law of hydration that specifies the evolution of degree of hydration x :

$$\frac{dx}{dt} = \tilde{A}(x) \exp\left(-\frac{E_a}{RT}\right) \quad (2)$$

in these expressions:

- C is the volumic calorific capacity;
- $K = K \mathbf{1}$ is the tensor of isotropic conductivity coefficients;
- I is the exchange coefficient on the contour;
- T_{imp} is the temperature imposed from the outside on the contour;
- $I > 0$ is the supposed constant hydration heat per degree of hydration unit, which is determined in TEXO on the basis of a calorimetric test;
- E_a / R is the Arrhenius constant;
- $\tilde{A}(x)$ is the normalized affinity, which depends solely on the degree of hydration x and the composition of the concrete used. This function is determined in TEXO on the basis of a calorimetric test.

The TEXO module thus leads to determining both the temperature and degree of hydration fields; it allows incorporating the effects of heat treatment (e.g. stoving, the installation of insulating tarpaulin or heating resistors). Besides these various solutions intended to minimize gradients, this time-

dependent module enables highlighting the influence of the date of formwork removal. Furthermore, it is also possible to simulate the subsequent concreting on an older concrete.

2.2. The "QAB" calorimetric test

The entire set of computations relies on the calorimetric test results, which are to be provided as input data. This test consists of recording the temperature curve of a concrete sample placed in a calorimeter vs. time. Figure 2 shows the curve under adiabatic conditions ($-\text{div } \mathbf{q} = 0$) for both an ordinary B25 concrete with a water/cement (W/C) ratio of 0.6 and a high performance B80 concrete with a W/C ratio of 0.4. In the TEXO module, these results serve to sample the function $\tilde{A}(\mathbf{x})$, by means of the following:

$$\tilde{A}(\mathbf{x}) = \frac{1}{T_{\infty}^{\text{ad}} - T_0} \frac{dT^{\text{ad}}(t)}{dt} \exp\left\{ \frac{E_a}{RT^{\text{ad}}(t)} \right\} \quad (3)$$

with respect to the degree of hydration, as determined from:

$$x = \frac{T^{\text{ad}}(t) - T_0}{T_{\infty}^{\text{ad}} - T_0} \quad (4)$$

With:

- $T^{\text{ad}}(t)$, temperature history, as measured in the adiabatic test,
- T_0 initial temperature of the sample,
- T_{∞}^{ad} asymptotic temperature.

Figure 3 displays the so-called "normalized affinity" $\tilde{A}(\mathbf{x})$ functions for the two concretes depicted in Figure 2, as determined using the TEXO module. It is to be noted that the peak of the curve $\tilde{A}(\mathbf{x})$, which corresponds to the inflection point of the curve $T^{\text{ad}}(t)$, rises with the decrease in W/C ratio, thereby generating a greater production of hydration heat at an early age in high performance concrete structures. The normalized affinity $\tilde{A}(\mathbf{x})$ also enables intrinsically characterizing the macroscopic hydration kinetics of the concrete used; this comes into play via the kinetic law (2) in the heat equation (1a) as a volume-based term of heat $I \, dx / dt$ due to the exothermal nature of the hydration reaction, with:

$$I = C(T_{\infty}^{\text{ad}} - T_0) > 0 \quad (5)$$

where I is the hydration heat per degree of hydration unit.

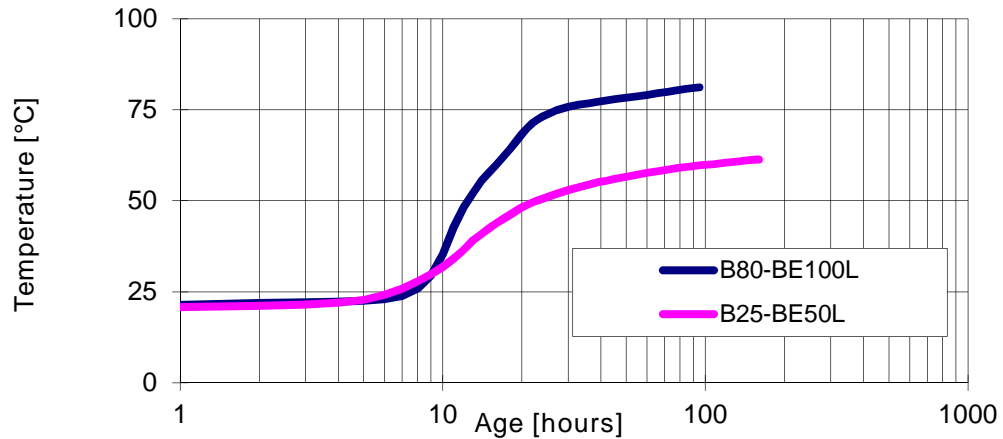


figure 2: Temperature histories $T^{\text{ad}}(t)$ measured in an adiabatic test for both an ordinary (B25) concrete and a high performance (B80) concrete $T^{\text{ad}}(t)$.

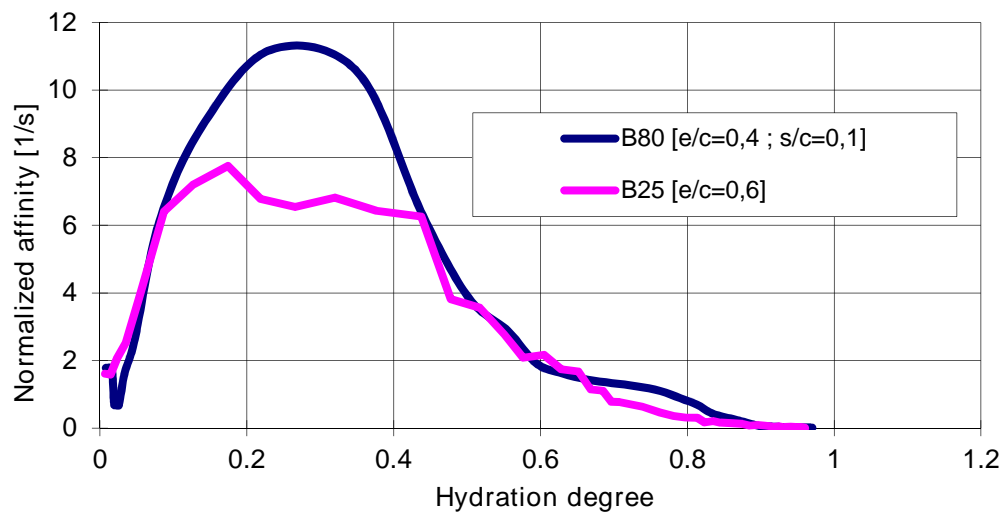


figure 3: $\tilde{A}(x)$ functions determined using the TEXO module for both an ordinary (B25) concrete and a high performance (B80) concrete ($E_a/R = 4,000 K$).

2.3. Boundary conditions

Thanks to the finite element method, it is possible to draw a general distinction between two types of boundary conditions:

- imposed flow,
- imposed temperature

Type 1: imposed flow (linear exchange):

The "imposed flow" type of boundary conditions using TEXO are most often associated with a linear exchange condition and allow incorporating heat losses through formworks, free surfaces, etc. This type of condition is of the following form:

$$q \cdot n = l(T - T_{\text{imp}}) = l(q - q_{\text{imp}}(t)) \quad (6a)$$

with I being the exchange coefficient on the contour, where the temperature $q_{\text{imp}}(t) = T_{\text{imp}}(t) - T_0$ is imposed and T_0 is the initial temperature.

Type 2: imposed temperature:

The "imposed temperature" type of boundary conditions allows imposing one (or several) temperature histories known at one or several mesh nodes (e.g. cooling tubes). These conditions take on the following form:

$$q(x, t_i) = q_{\text{imp}}^i(x, t)$$

Moreover, it is also possible to transform, at any time step, a type (2) "imposed temperature" boundary condition into a type (1) "imposed flow" boundary condition, and vice versa.

Initialization of the temperature field:

Besides the type 1 and 2 boundary conditions, running the TEXO module necessitates initializing the temperature field, such that:

$$q(x, t=0) = q_0(x) \quad (6b)$$

For this purpose, an option has been included in the data set of the TEXO module; this option serves to initialize the nodal values of temperature on the basis of any input values. Such input may eventually be read from a file or initialized from a previous computation, either with the DTLI module (steady-state solution) or with the TEXO module itself (phase-by-phase construction). If the INI option is not used, the CESAR code initializes nodal temperatures at 0°C.

3. MODULE MEXO

3.1. Theoretical and experimental aspects

The MEXO module has primarily been set up as an incremental elastic mechanical resolution module with displacement-based (and eventually loading-based) boundary conditions, in which both dilatation and heat shrinkage / chemical shrinkage are taken into account.

Subsequent to a computation using the TEXO module, it is possible (with the help of MEXO):

- to determine the mechanical effects (displacements, stresses) of the evolution in both temperature and degree of hydration in early-age concrete structures
- to predict the risk of cracking.

Note that $de = de + de/3I$ is the strain increment tensor. The constitutive law used for early-age concrete is written in the following incremental form:

$$ds = \frac{E(x)}{1+n} de + \frac{E(x)}{3(1-2n)} (de - 3adT - 3bdx)I \quad (7)$$

where:

- $E(x)$ is the modulus of elasticity, which depends on both the degree of hydration (hardening) and Young's modulus of the hardened material;
- n is Poisson's ratio of the concrete (assumed constant);
- a is the coefficient of dilatation per unit length of concrete (assumed constant);

- b is the coefficient of dilatation / chemical shrinkage of the concrete (assumed constant)

3.2. Concrete hardening

As regards the evolution of the modulus $E(x)$, Byfors' law has been adapted for MEXO and placed in the following form:

$$E(x) = E(\%)f(x) \quad (8a)$$

with:

$$f(x) = \frac{1 + 1,37R_c(\%)^{2,204}}{1 + 1,37R_c(x)^{2,204}} \left(\frac{R_c(x)}{R_c(\%)} \right)^{2,675} \quad (8b)$$

$$R_c(\%) = \frac{1}{7250} \frac{E(\%)^{0,471}}{E(x)^{0,471}} \quad (8c)$$

where:

- $E(\%)$ [in MPa] is Young's modulus of the hardened material;
- $R_c(\%)$ [in MPa] is the compressive strength of the hardened material, and $R_c(x)$ its evolution as a function of the degree of hydration x .

To carry out this adaptation procedure, a bilinear relation is introduced, such that:

$$R_c(x) = \begin{cases} xR_{co} & \text{si } x \leq x_0 \\ R_{co} + \frac{(R_c(\%) - R_{co})(x - x_0)}{1 - x_0} & \text{si } x > x_0 \end{cases} \quad (9)$$

where x_0 is the "threshold" of the hardened material (i.e. the degree of hydration from which point forward the material may be considered as a solid).

Application of Byfors' law in the form of (8a-c) and (9) serves to reduce the data necessary for modelling hardness to:

- $E(\%)$: Young's modulus of the hardened material;
- x_0 : Threshold of the hardened material (= degree of hydration at the time of setting).

Figure 4 shows the evolution in Young's modulus vs. degree of hydration for both an ordinary concrete (OC) and a high performance concrete (HPC), as determined with Byfors' law and then compared with the experimental values.

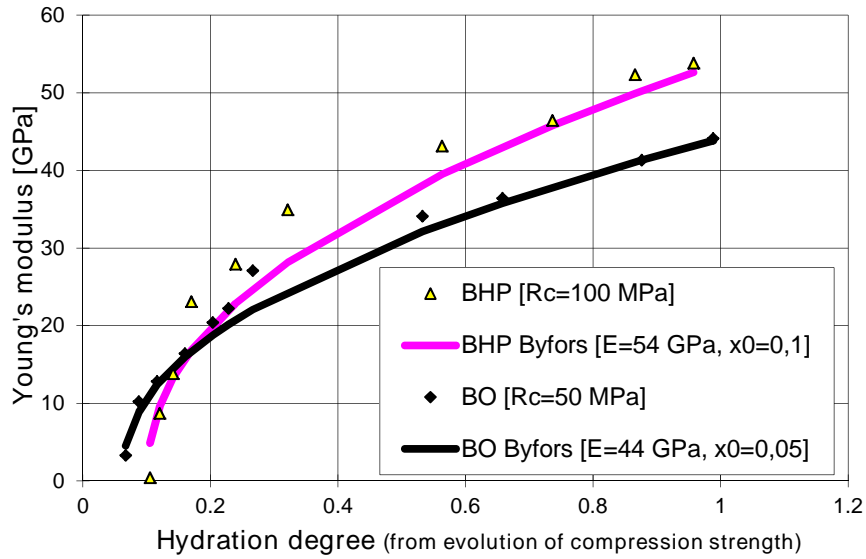


Figure 4: Evolution in Young's modulus during early age, according to Laplante's experimental values (1993) and Byfors' law used in the MEXO module, for both an ordinary concrete (OC, W/C = 0.5) and a high performance concrete (HPC, W/C = 0.3; S/C = 0.1).

3.3. Coefficient of dilatation/chemical shrinkage

By denoting $ds = ds + ds_I$, equation (7) can be inverted as follows:

$$de = \frac{a(1+n)}{E(x)} ds + \frac{1-2n}{E(x)} ds_I + adT + bdx_I$$

$de = bdx_I$ is identified as the incremental strain caused by the degree of hydration unit dx , and b as the coefficient of chemical dilatation. b is positive in the case of unrestricted and isothermal chemical swelling, and negative in the case of shrinkage.

For early-age concrete, this coefficient governs the incorporation of endogenous shrinkage in MEXO and ultimately proves to be non-constant, as conveyed in figure 5, which shows the evolution in endogenous shrinkage vs. degree of hydration for both concretes presented in Figure 3. As part of an initial approach, this coefficient is assumed constant in MEXO, thus coinciding with the total endogenous shrinkage recorded for a concrete. This approach then leads, for small degrees of hydration, to overestimate endogenous shrinkage.

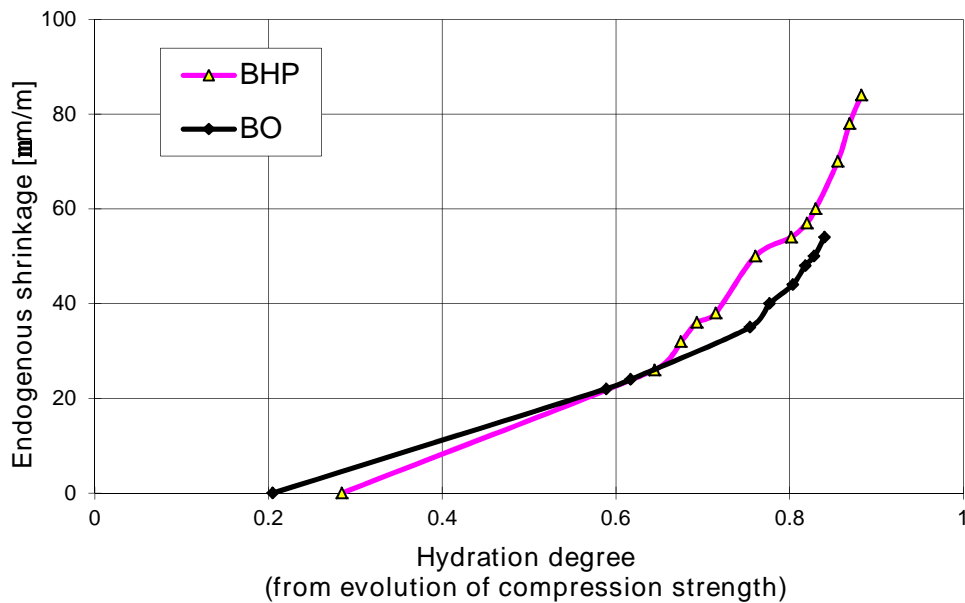


figure 5: Evolution of endogenous shrinkage for both an ordinary concrete (OC, $W/C = 0.5$) and a high performance concrete (HPC, $W/C = 0.3$; $S/C = 0.1$) [experimental values developed by Laplante (1993)]

4. RESULT OF A "QAB" CALORIMETRIC TEST

A key data component in computations involving the TEXO module is the result of a calorimetric test (see Section 1.2.1). The calorimetric test data for TEXO are the following:

- temperature history $q(\dot{t})$ of the sample [in °C];
- temperature history $q^{\text{ext}}(\dot{t})$ outside the calorimeter [in °C];
- calibration coefficients A, B, C for losses due to the calorimeter used,
- volumic calorific capacity $CM = C$ of the sample volumic calorific capacity $CM = C$ of the sample;
- Arrhenius' constant: $XK = E_a/R$.

Perfectly-adiabatic test

In the case of a perfectly-adiabatic test (without any calorimeter-related heat losses), the temperature outside the calorimeter is equal to the initial temperature of the outside sample, $q^{\text{ext}}(t) = q(0) = \text{constant}$. Moreover, for the calibration coefficients of calorimeter losses, the following are to be used:

$$\mathbf{A = 0, B = 0, C = 1.}$$

Essai dit « quasi-adiabatique » (QAB)

Dans le cas d'un essai quasi-adiabatique avec des pertes du calorimètre, les histoires de température de l'échantillon, $q(\dot{t})$, et de température extérieure, $q^{\text{ext}}(\dot{t})$, sont mesurées. Les coefficients d'étalonnage des pertes du calorimètre utilisés A, B, C, sont fournis avec le résultat de l'essai.

So-called "quasi-adiabatic" (QAB) test

In the case of a quasi-adiabatic test with calorimeter losses, the histories of both the sample temperature, $q(t)$, and the outside temperature, $q^{\text{ext}}(\dot{t})$, are measured. The calibration coefficients of calorimeter losses A, B, C are provided with the test result

Calorific capacity of the sample

The CM parameter corresponds to the volumic calorific capacity C of the sample (i.e. of the concrete used); the value listed in Table II will be employed herein, while respecting the units used in the computation.

Arrhenius' constant

The XK parameter represents Arrhenius' constant E_a/R . In the absence of more precise information, set **XK = E_a/R = 4000 K**. Nonetheless, this value may vary from 4000 to 7000, especially at very early age.

5. TEXO-MEXO IN EXAMPLE: CONCRETING STAGES AND THERMAL TREATMENT

5.1. Introduction

This example simulates a phasing of the concreting (broken down into two phases), followed by heat treatment (see figure 6). This requires the sequencing of three computations:

- 1st computation: First concreting stage, the first solid block is cast and the formwork is removed after 12 hours.
- 2nd computation: Second concreting stage: a second solid block is cast on both sides of the first one. The two parts of the second block are also stripped of their formwork after 12 hours.
- 3rd computation: In order to protect against the consequences of thermal gradients, hot air at 30°C is blown over all exterior surfaces of the concrete newly removed from its formwork

The problem geometry (see figure 9) exhibits a plane of symmetry Oyz that is also respected by the evolution in material characteristics, boundary conditions and the loading. Therefore only half of the structure needs to be modelled.

The meshing finally carried out is drawn figure 12. The material groups and

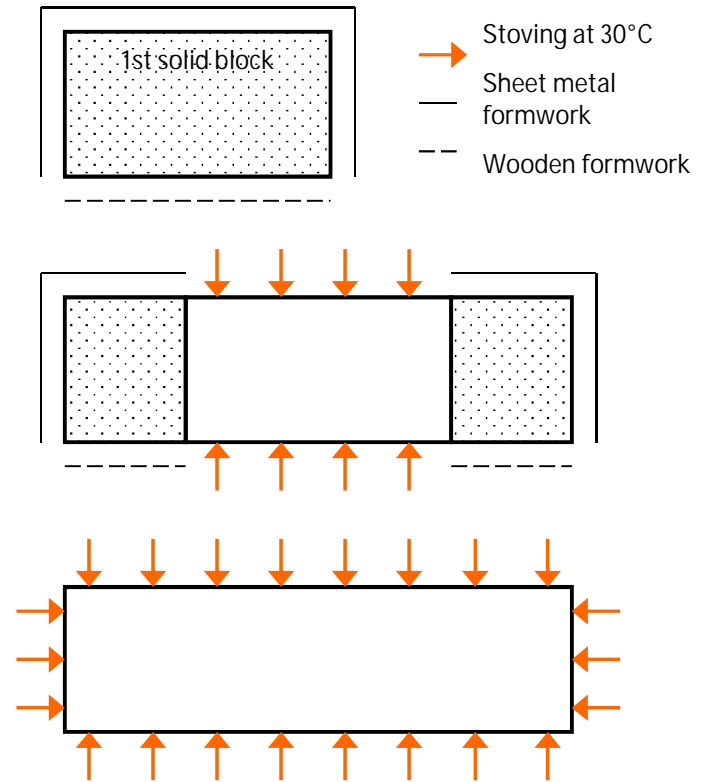
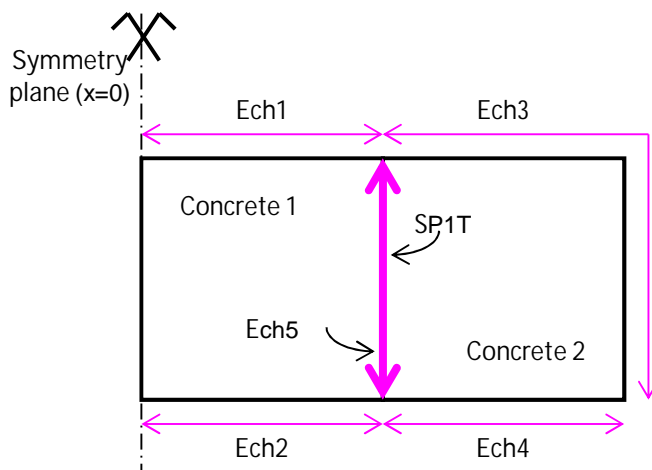


figure 6: Analyzed problem - Geometry



exchange conditions (set as boundary conditions) are shown hereafter.

figure 7a: TEXO modelling setup

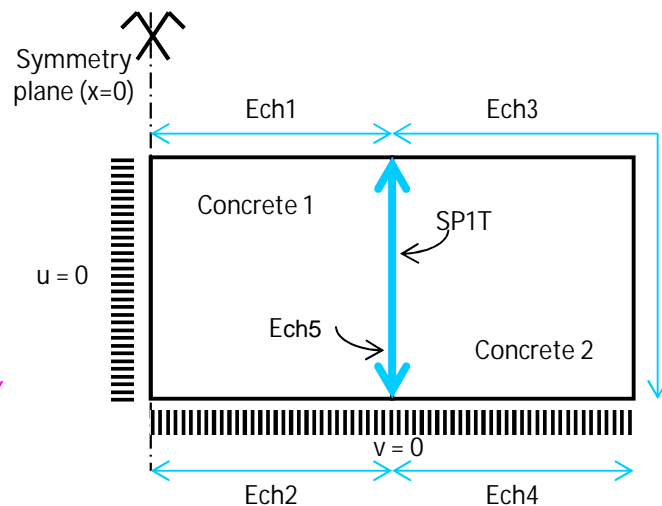


figure 7b: MEXO modelling setup

Table 1: Evolution in the characteristics of the various element groups for TEXO calculations (units: [m, W, hr])

N°	Name	Stage #1	Stage #2	Stage #3
1	Concrete 1	AKX = 6. AKY = 6. AKXY = 0. CC = 2400.	è	è
4	Concrete 2	idem Concrete 1	è	è
2	Exchange: Ech1	ECH = 15.	ECH = 34. ¹	è
3	Exchange: Ech 2	ECH = 12.	ECH = 34.	è
5	Exchange: Ech 3	ECH = 0.0	ECH = 15.	ECH = 34.
6	Exchange: Ech 4	ECH = 0.0	ECH = 12.	ECH = 34.
8	Exchange: Ech 5	ECH = 15.	ECH = 0.	è
7	Special elements: SP1T	K = [0]	$K = \begin{pmatrix} \hat{e}10^9 & -10^9\hat{u} \\ \hat{e} & 10^9\hat{t} \end{pmatrix}$	è

The symbol è indicates that the characteristics of the group remain unchanged from the previous computation.

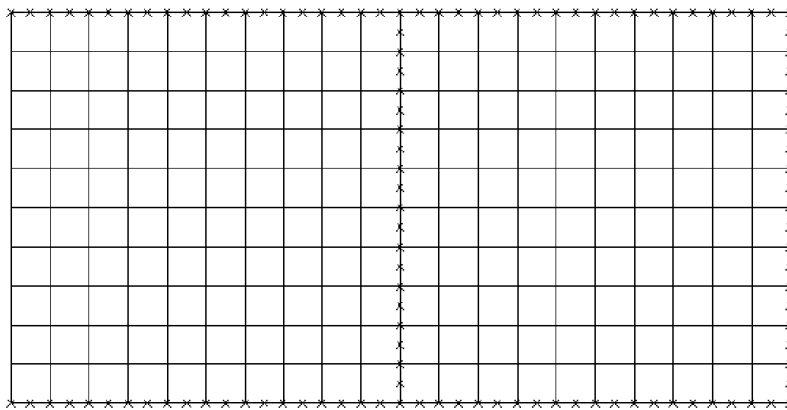


figure 8: view of the mesh

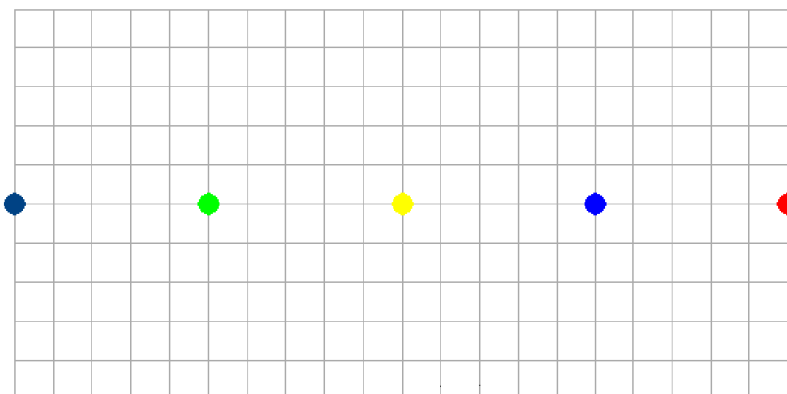


figure 9: Situation of points followed for the analysis of the calculation stages

¹ he = 9.45 corresponds to a free surface exposed to the hot air blown.

5.2. Some results of the TEXO analysis

Stage #1

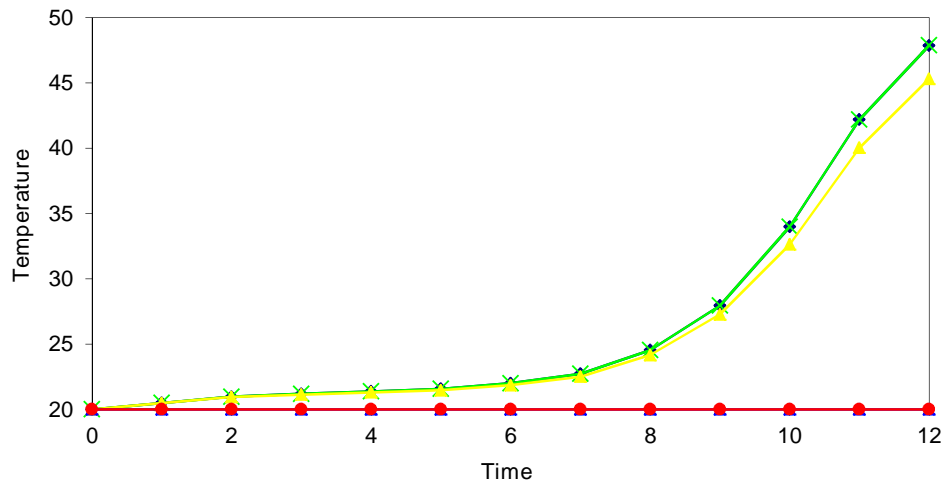


figure 9: Evolution of the temperature during stage #1

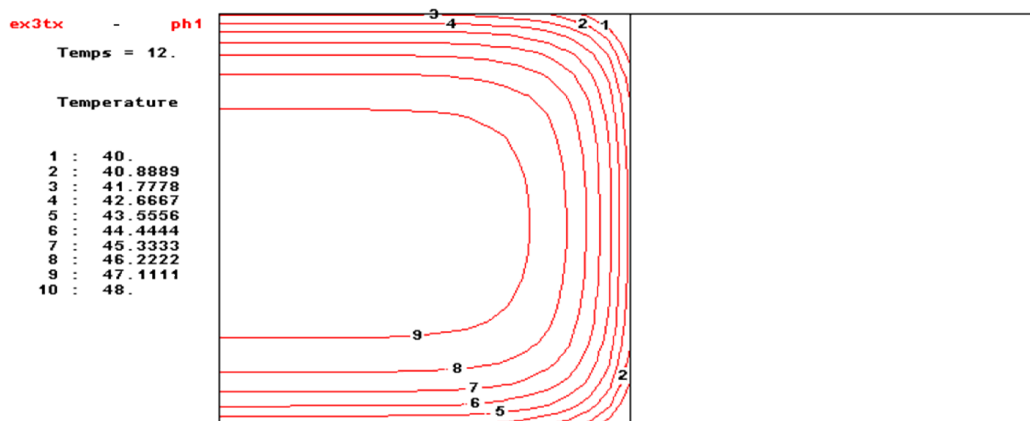


figure 10: Isocurves of temperature at t=12h

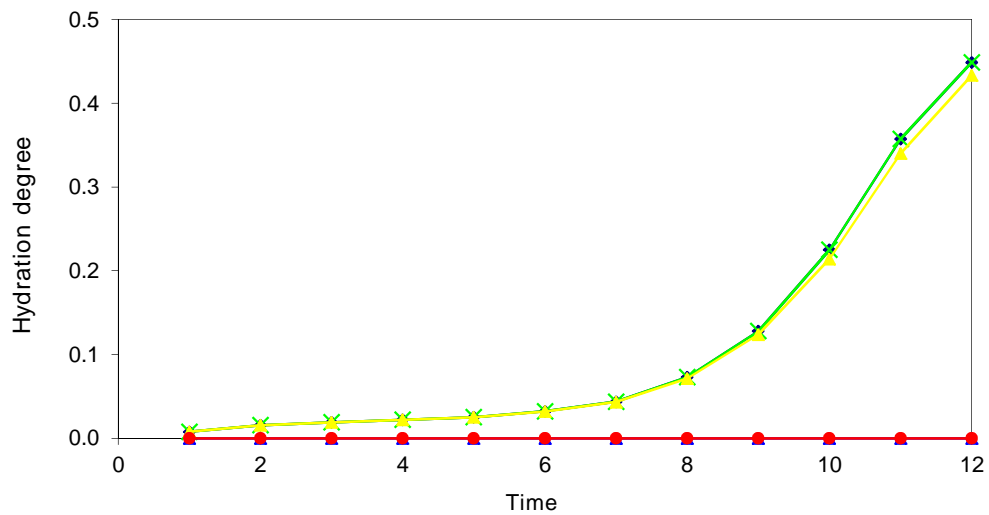


figure 11: Evolution of the hydration degree during stage #1

Stage #2

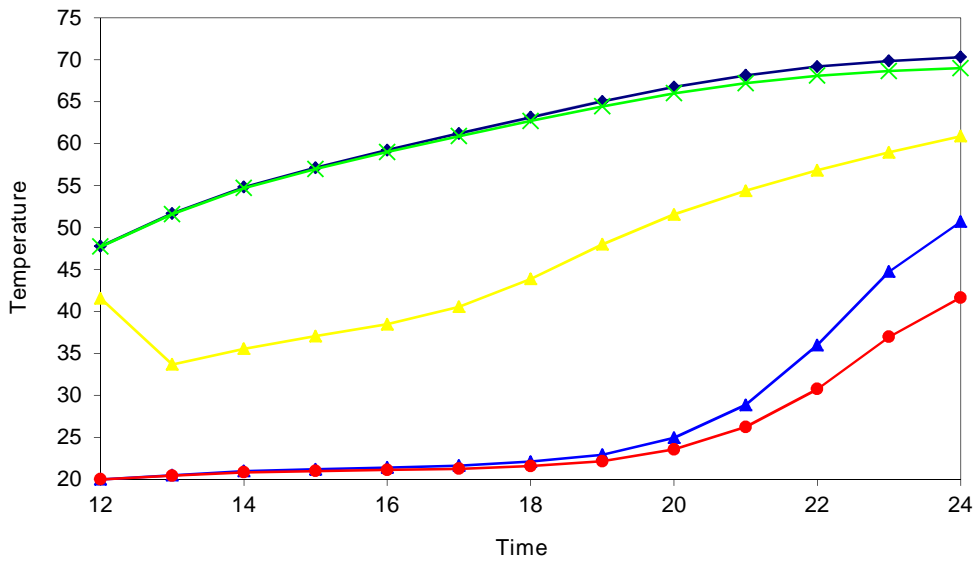


figure 12: Evolution of the temperature during stage #2

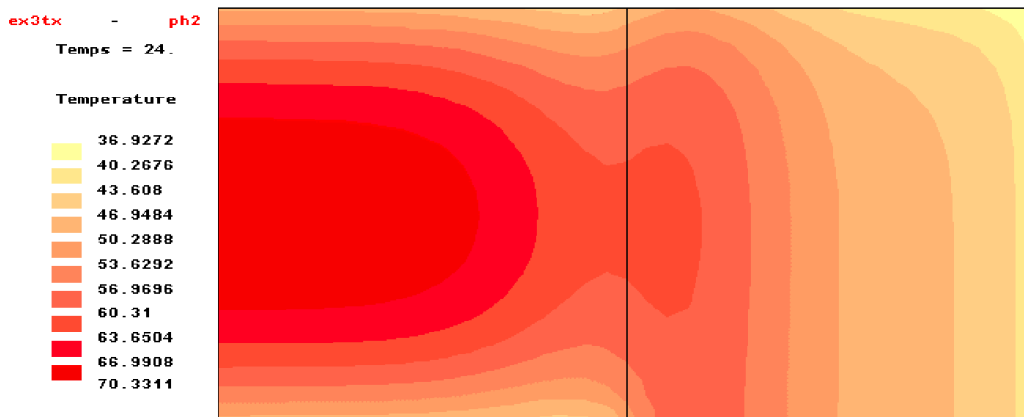


figure 13: Isovalues areas of temperature at t=24h

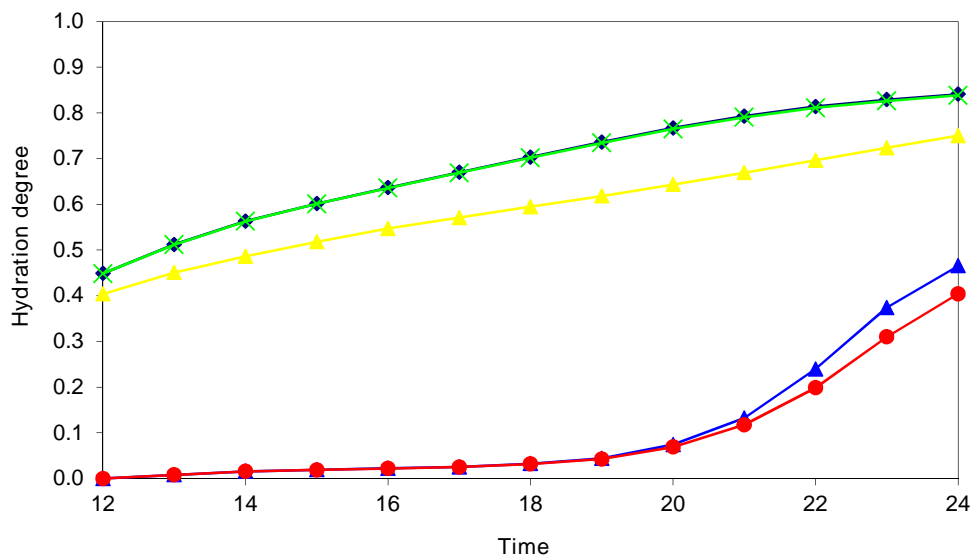


figure 14: Evolution of the hydration degree during stage #2

Stage #3

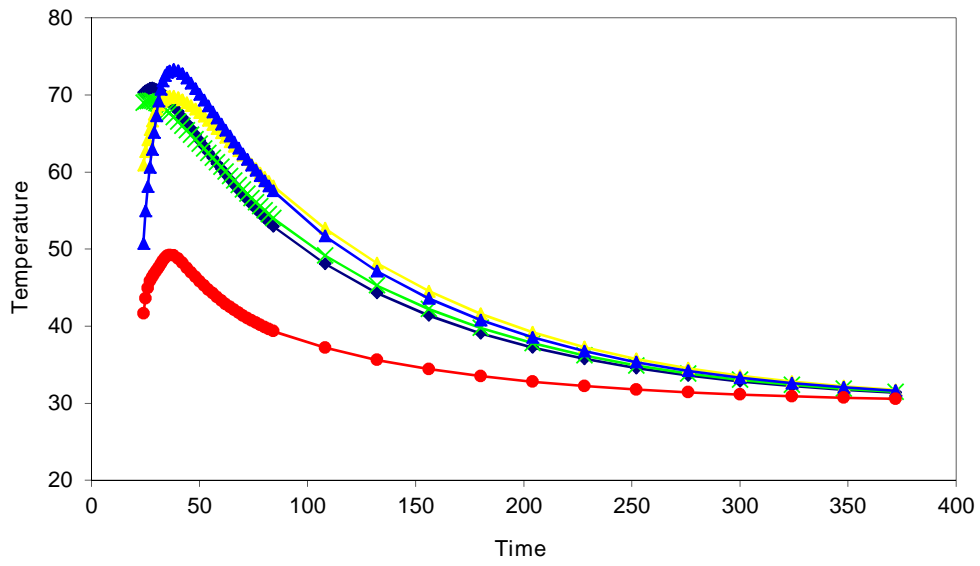


figure 15: Evolution of the temperature during stage #3

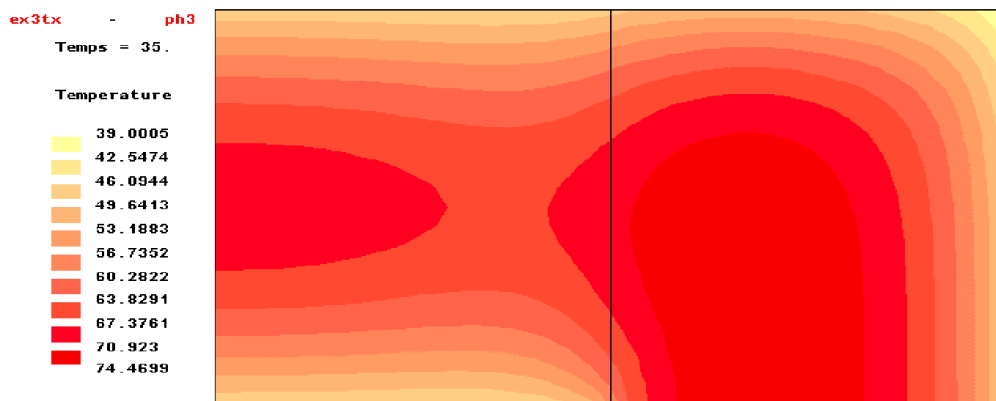


figure 16: isovalues areas of temperature at t=35h

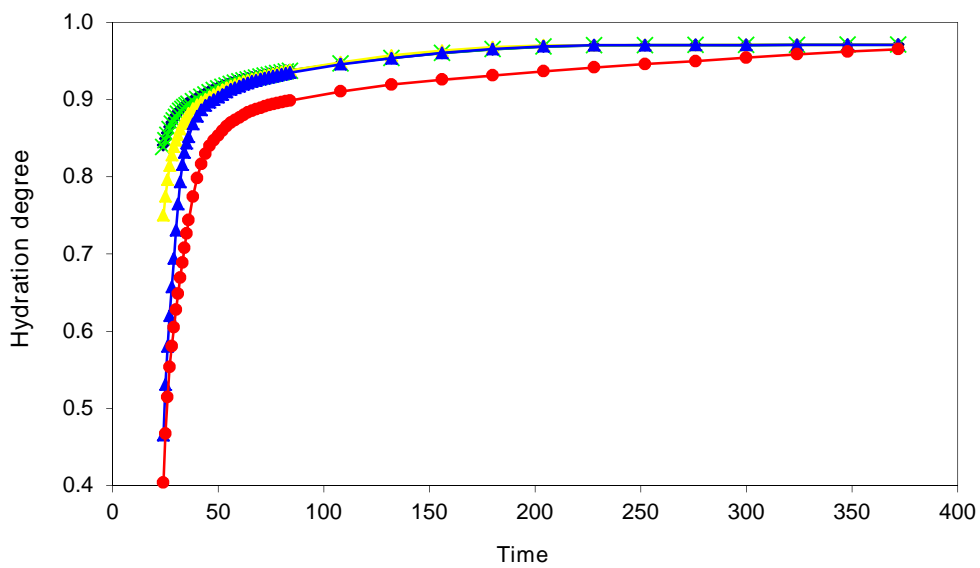


figure 17: Evolution of the hydration degree during stage #3

5.3. Some results of the MEXO analysis

Stage #1

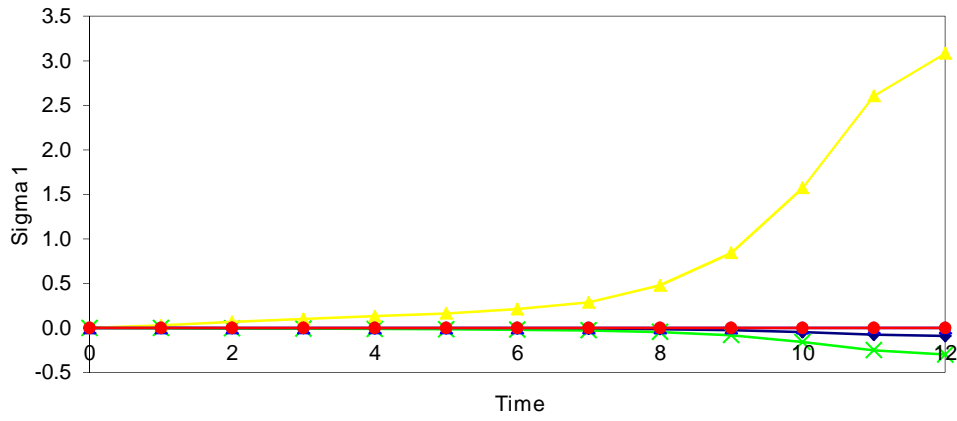


figure 18: Evolution of the main stress during stage #1

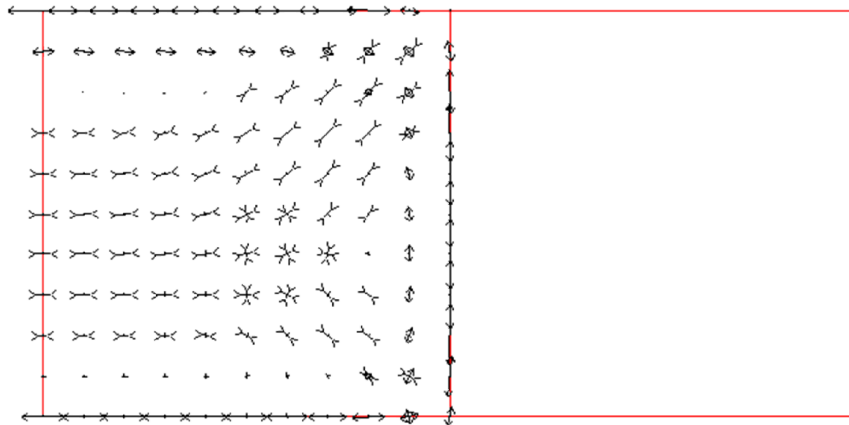


figure 19: Field of the main stresses S1 in the piece at t=12h

Stage #2

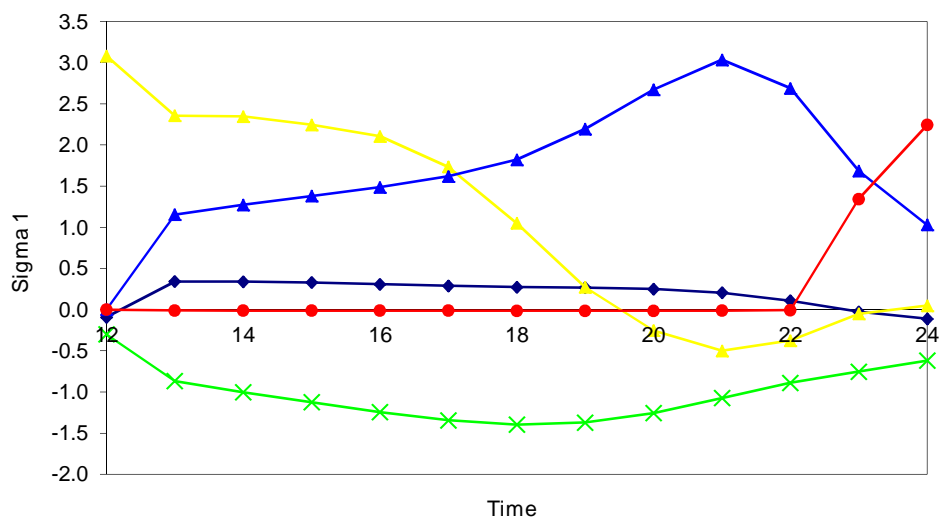


figure 20: Evolution of the main stress during stage #2

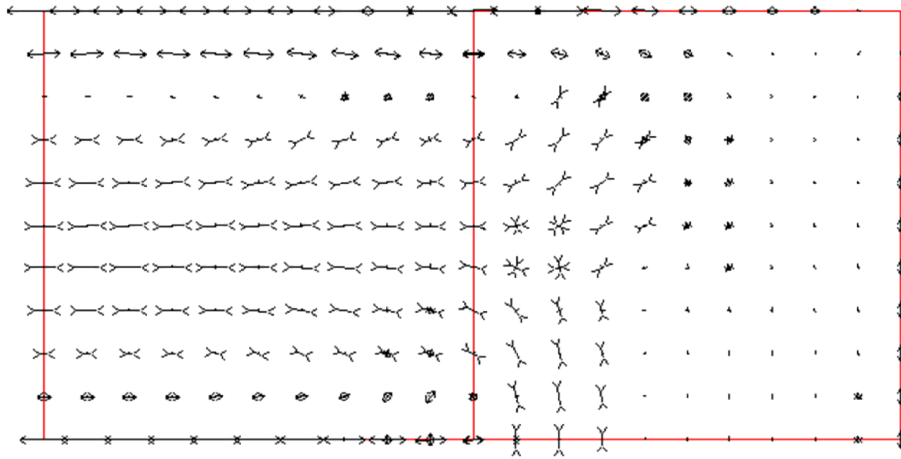


figure 21: Field of the main stresses $S1$ in the piece at $t=24h$

Stage #3

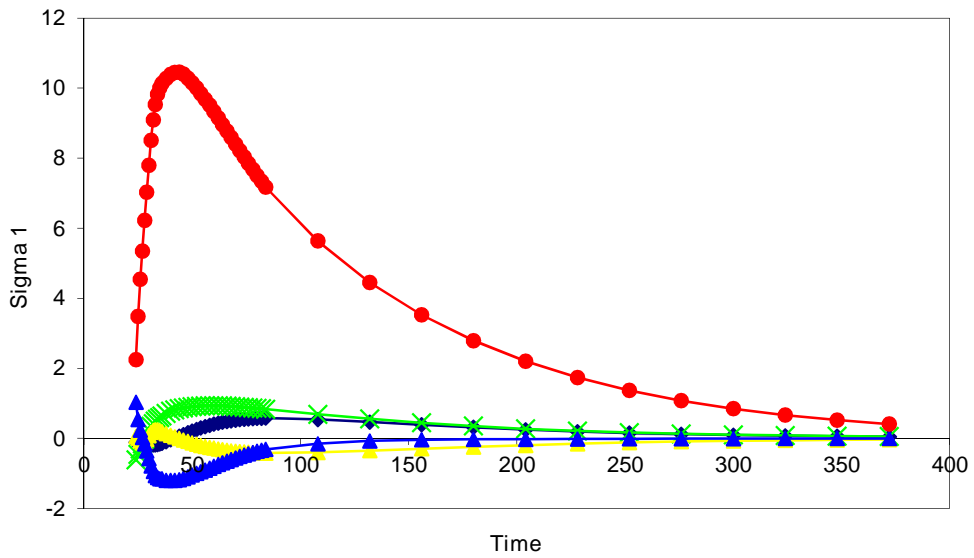


figure 22: Evolution of the main stress during stage #3

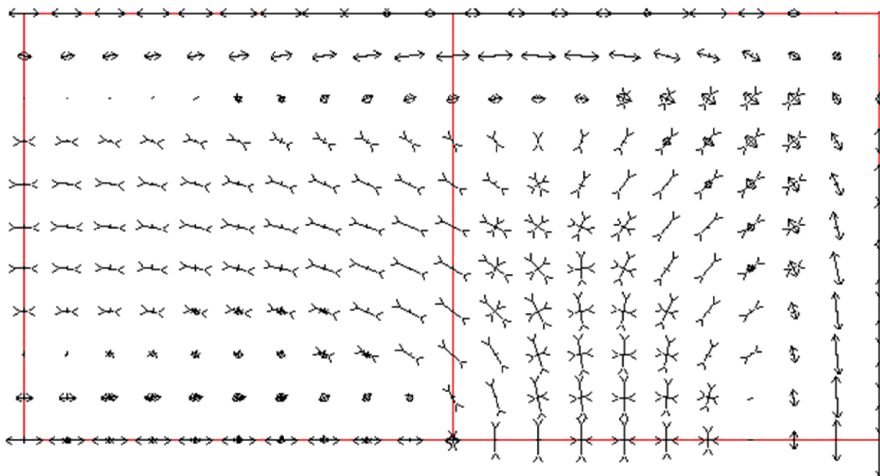


figure 23: Field of the main stresses $S1$ in the piece at $t=35h$

6. BIBLIOGRAPHICAL RÉFÉRENCES

ACKER P., PIAU J.M., RADOUANT I. (1987)

« *Modelling Thermal and Hygrometric Effects in Concrete* »

IABSE Colloquium, Delft, pp. 285-292.

de LARRARD F., ITHURRALDE G., ACKER P., CHAUVEL D. (1990)

« *High performance concrete for a nuclear containment* »

2nd International Conference on Utilization of High Strength Concrete, Berkeley

ACI SP 121-28.

ITHURRALDE G., de LARRARD F., NECTOUX J. (1991)

« *Bétons à hautes performances pour l'étanchéité des structures en béton - Expérimentation* »

Annales de l'ITBTP, n° 502, mars-avril 1992, pp 77-115.

LAPLANTE P. (1993)

« *Propriétés mécaniques des bétons durcissants : analyse comparée des bétons classiques et à très hautes performances* »

Collection Études et Recherches des Laboratoires des Ponts et Chaussées, série Ouvrages d'Art, référence OA13, Décembre 1993, 300 pages, ISBN 2-7208-2300-3

TORRENTI J.M., PATIES C., PIAU J.M., ACKER P., de LARRARD F. (1992)

« *La simulation numérique des effets de l'hydratation du béton* »

Colloque StruCoMe, Paris, 12 pages.

ULM F.J., COUSSY O. (1995a)

« *Modeling of thermochemomechanical couplings of concrete at early age* »

Journal of Engineering Mechanics, ASCE, Vol. 121, N° 7, pp. 785-794.

ULM F.J., COUSSY O. (1995b)

« *Strength growth on chemo-plastic hardening in early age concrete* »

Journal of Engineering Mechanics, ASCE, vol. 122, n°12, Dec. 1996, pp. 1123-1131.

DIDRY O., GRAY M.N., COURNUT A., and GRAHAM J. (2000)

« *Modelling the early age behaviour of a low heat concrete bulkhead sealing an underground tunnel.* »

Can. J. Civ. Eng./Rev. Can. Génie Civ., Vol. 27(1), pp. 112-125 (2000)

Edité par :



8 quai Bir Hakeim

F-94410 SAINT-MAURICE

Tél. : +33 1 49 76 12 59

cesar-lcpc@itech-soft.com

www.cesar-lcpc.com

Ó itech - 2015